

The Shrunken, Bright Cerebellum: A Characteristic MRI Finding in Congenital Disorders of Glycosylation Type 1a

CLINICAL REPORT

P. Feraco
M. Mirabelli-Badenier
M. Severino
M.G. Alpigiani
M. Di Rocco
R. Biancheri
A. Rossi

SUMMARY: CDG-1a is an early-onset neurodegenerative disease with selective hindbrain involvement and highly variable clinical presentation. We retrospectively reviewed the clinical records and MR imaging studies of 5 children (3 boys and 2 girls aged 12 days to 2 years at presentation) with molecularly confirmed CDG-1a. The cerebellum was hypoplastic at presentation in 4 cases, progressive bulk loss involved the cerebellum and the pons in all cases, and the cerebellar cortex and subcortical white matter were hyperintense on T2-weighted and FLAIR images in all. We conclude that CDG-1a likely results from a combination of cerebellar hypoplasia and atrophy. Cerebellar volume loss with diffuse T2/FLAIR hyperintensity seems to be a peculiar association in the field of cerebellar atrophies, and may be useful to address the differential diagnosis.

ABBREVIATIONS: BAEP = brain stem auditory evoked potential; CA = cerebellar atrophy; CDG = congenital disorders of glycosylation; CH = cerebellar hypoplasia; EEG = electroencephalogram; ERG = electroretinogram; mIns = myo-inositol; NCV = nerve conduction velocity; PMM = phosphomannomutase; PRESS = point-resolved spectroscopy sequence; sl = scyllo-inositol; VEP = visual-evoked potentials

CDGs are genetically heterogeneous autosomal recessive disorders caused by abnormal glycosylation of N-linked oligosaccharides. CDG-1a (OMIM#212065), caused by mutation in the gene encoding *PMM2*, is the most common form. The clinical presentation and course are highly variable, ranging from severe infantile multisystem involvement to mild late-onset forms.¹ Muscular hypotonia, strabismus, and developmental delay are variably associated with dysmorphic features, abnormal subcutaneous fat distribution (“fat pads”), nipple retraction, feeding problems, and failure to thrive.² Stroke-like episodes have also been reported.³ Brain MR imaging studies have consistently shown a small cerebellum, variably designated as cerebellar hypoplasia, olivopontocerebellar hypoplasia, or cerebellar atrophy.³⁻⁷ The purpose of this study is to describe the MR imaging findings on initial and follow-up studies in patients with CDG-1a and to identify suggestive MR imaging features that may prompt further diagnostic tests.

Materials and Methods

Institutional review board approval was not sought, as it is not required in our country for retrospective studies that do not involve patient identity disclosure. Five Italian children (3 males and 2 females, aged 12 days to 2 years at clinical presentation) with confirmed CDG-1a constitute the focus of this article. These patients were selected on the basis of a molecular genetic confirmation of the diagno-

sis and the availability of at least 1 MR imaging study for evaluation. We retrospectively reviewed their clinical, laboratory, electrophysiologic, and neurologic information. Laboratory investigations included routine blood work, analysis of transferrin by serum isoelectric focusing, and enzymatic analysis of *PMM2* activity on skin fibroblasts. In all cases, molecular analysis of the *PMM2* gene was performed according to standard techniques. NCV studies were performed on all patients; VEPs, ERGs, and EEGs were performed in 4, whereas BAEPs were performed in 3.

A total of 9 brain MR imaging studies were performed in the 5 patients between 1991 and 2008; each patient underwent 2 MR imaging studies, except patient 2. The interval between the 2 MR imaging studies in individual patients ranged from 10 months to 14 years. Of the 9 MR imaging studies, 8 were performed with a 1.5T superconductive system (Intera Achieva; Philips, Best, the Netherlands) using an 8-channel parallel imaging head coil; these studies included 3-mm-thick sagittal T1- and T2-weighted images, 5-mm-thick axial T1- and T2-weighted images, and 4-mm-thick coronal T2-weighted and FLAIR images. Imaging parameters were as follows: TR 500–670 ms, TE 12–25 ms, NEX 2, for T1 weighting; TR 3500–5580 ms, TE 100–140 ms, and NEX 2, for T2 weighting; and TR 11,000 ms, TE 140 ms, TI 2800 ms, and NEX 2, for FLAIR. Gadolinium chelate was not administered. DWI was obtained with a single-shot echo-planar imaging technique (b-value, 0 and 1000 seconds/mm²) on either axial or coronal planes with automatic generation of ADC maps. Raw data were available for retrospective ADC value calculation in 4 examinations (Table); in these cases, cerebellar ADC was estimated by manually drawing 3 rounded 60-mm² regions of interest over the vermis and each cerebellar hemisphere, and by calculating the average of the 3 values obtained. In the remaining 5 MR examinations, DWI and ADC maps were visually assessed for the presence of areas of restricted or increased diffusion, but quantitative measurements could not be made. In 4 cases, ¹H-MRS was performed using a single-voxel PRESS technique at short (23–32 ms) TE; a 18 × 18 × 18 mm volume of interest was manually placed on the right cerebellar hemisphere, and the spectra were processed with built-in software providing automatic peak assignment and ratio calculation. Only 1 MR imaging

Received February 7, 2012; accepted after revision February 26.

From the Departments of Pediatric Neuroradiology (P.F., M.S., A.R.), Infantile Neuropsychiatry (M.M.-B., R.B.), Pediatrics (M.G.A.), and Pediatrics II (M.D.R.), G. Gaslini Children's Hospital, Genova, Italy.

P.F. and M.M.-B. contributed equally to the manuscript.

Previously presented as a preliminary report at: 44th Annual Meeting of the American Society of Neuroradiology, May 1, 2006; San Diego, California.

Please address correspondence to Andrea Rossi, MD, Department of Pediatric Neuroradiology, G. Gaslini Children's Hospital, Largo G. Gaslini 5, 16147 Genova, Italy; e-mail andrearossi@ospedale-gaslini.ge.it

<http://dx.doi.org/10.3174/ajnr.A3151>

MRI findings in 5 patients with CDG-1a					
Patients	1	2	3	4	5
Gender	M	F	M	M	F
Age at first MRI	12 days	5 months	2 years	7 months	9 months
Age at second MRI	11 months	NA	16 years	2 years	3 years
Cerebellar volume loss at presentation	Mild	Severe	Severe	Moderate	Mild
Progressive cerebellar atrophy on follow-up	Yes	NA	Yes	Yes	Yes
Cerebellar T2/FLAIR hyperintensity	Yes	Yes	Yes	Yes	Yes
Small pons	Yes (only on follow-up)	Yes	Yes (progressive on follow-up)	Yes (progressive on follow-up)	No
Pons size, sagittal x coronal (mm × mm)	13 × 19 (first MRI) 12 × 19 (second MRI)	13 × 19	NA	NA	19 × 27 (second MRI)
Supratentorial involvement	Delayed WM myelination, ventriculomegaly	No	Cortical atrophy, WM atrophy and gliosis, ventriculomegaly	No	No
DWI findings, cerebellum (s/mm ²)	↑ ADC 1.589 (first MRI) 1.665 (second MRI)	↑ ADC 1.238	NA	NA	↑ ADC 1.032 (second MRI)
¹ H-MRS findings (cerebellum)	NA	Quality insufficient	↓ NAA/Cr	↑ ml/Cr ↑ sl/Cr ↓ Cho/Cr ↓ NAA/Cr ↑ αGlx	↑ ml/Cr ↓ Cho/Cr ↓ NAA/Cr

Note:—αGlx: alpha-glutamine/glutamate complex; NA, not available.

study, performed 20 years ago in patient 3, was performed on a first-generation 0.5T magnet, which only allowed for 5-mm thick T1- and T2-weighted images to be obtained. Findings on both conventional and advanced MR imaging modalities were compared with a data base developed at our institution consisting of normal age-matched controls.

Regarding the methods of retrospective analysis, given the small size of the series, it was decided that a consensus analysis by 2 experienced neuroradiologists (P.F. and A.R.) was sufficient. The degree of cerebellar volume loss was arbitrarily assigned as mild, moderate, or severe; presence of cerebellar signal abnormalities and progressive volume loss on follow-up were recorded as present or absent. Pontine size was calculated as previously reported⁸ in 4 cases (Table); in the remaining 5, objective measurements were not available and pontine volume was subjectively assessed. Associated supratentorial findings were noted.

Results

Clinical, Neurophysiologic, Laboratory, and Molecular Findings

All children were born at term from healthy, unrelated parents after uncomplicated pregnancies and deliveries. Three subjects presented with muscular hypotonia, feeding difficulties, and failure to thrive, either in the neonatal period (cases 1 and 2) or in the second month of life (case 3). Case 4 presented with renal and hepatic involvement at 3 months, and case 5 with developmental delay at 7 months. Facial dysmorphism, inverted nipples, and fat pads were observed in 4 patients, hepatomegaly in 2 (cases 3 and 4), and renal cortical hyperchogenicity in 3 (cases 2–4). Neurologic examination showed strabismus, muscular hypotonia, and weakness in all children, with poor tendon reflexes related to peripheral neu-

ropathy in 4. Laboratory investigations showed elevated transaminases in all patients as well as a type I transferrin isoform pattern at isoelectric focusing of serum transferrin. The diagnosis of infantile type CDG-1a was confirmed by significantly decreased PMM activity in fibroblasts and by the presence of *PMM2* mutations in all patients. Neurophysiologic study showed slowing of motor NCV in 4 patients (cases 1, 3, 4, and 5), and normal NCV in the remaining patient at 15 months of life; reduced amplitude of VEP/ERG was found in 2 subjects (cases 2 and 3), and normal VEP/ERGs were found in 2 (cases 4 and 5); sensorineural abnormality at BAEP was found in 1 (case 3), whereas BAEPs were normal in the remaining 2 (cases 4 and 5). EEGs showed slow background activity in 2 patients (cases 1 and 3) and was normal in the other 2 (cases 2 and 5).

MR Imaging Findings

MR imaging findings are summarized in the Table. A variably severe reduction in size of the cerebellar folia, involving both the vermis and the hemispheres, with corresponding enlargement of the fissures was present in all patients (Fig 1). In 1 of them (case 1), MR imaging during the neonatal period showed inferior vermis hypoplasia, progressing to diffuse cerebellar volume loss on follow-up (Fig 2). In all patients in whom follow-up studies were available for review (cases 1, 3, 4, 5), the MR imaging examinations showed worsening, with progressive cerebellar volume loss (Fig 3). Careful analysis of vermis morphology showed that the volume of the superior vermis appeared to reduce uniformly, with a corresponding degree of folial diminution and fissural enlargement. In 4 cases (cases 1–4), the inferior vermis had a flat appearance both at presentation and on

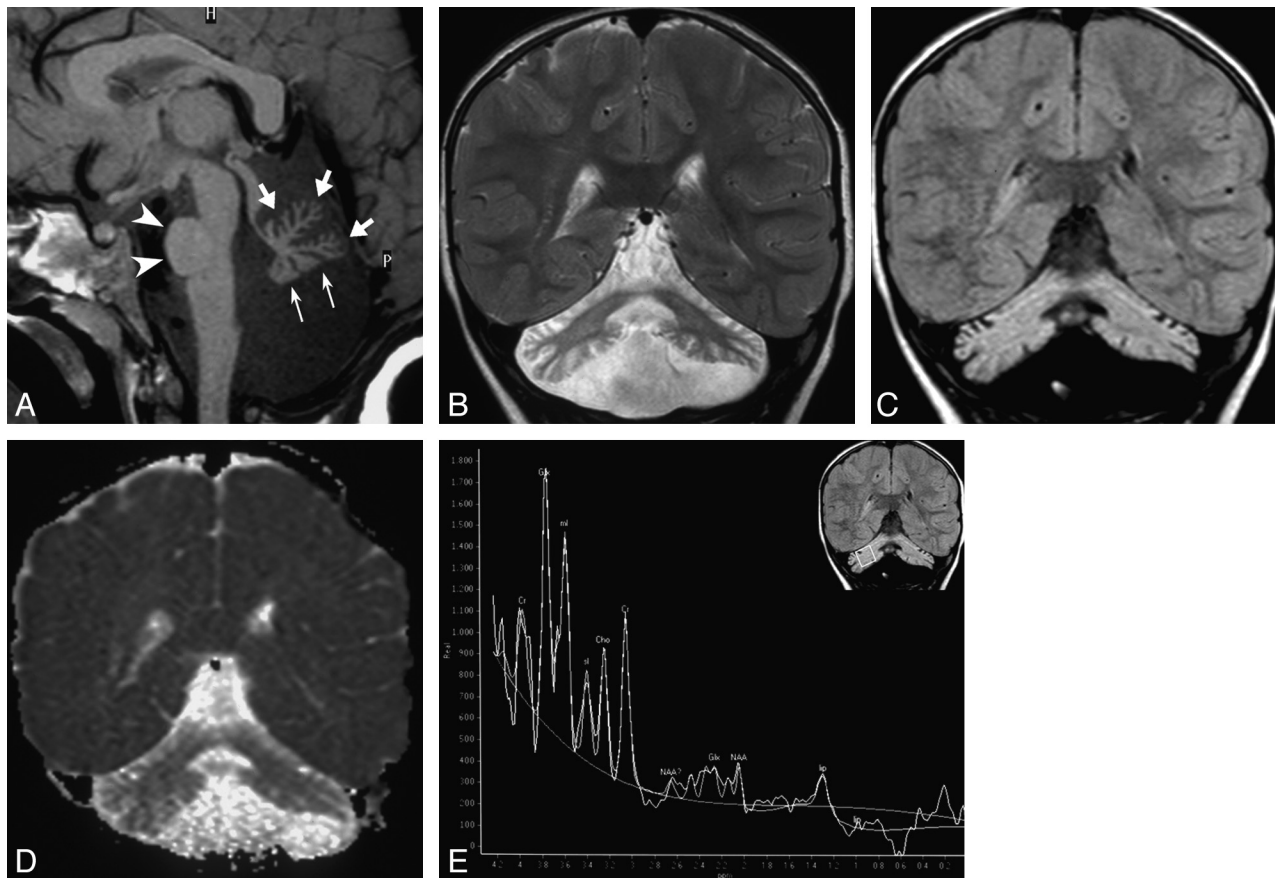


Fig 1. Typical MR imaging findings in CDG-1a; case 4 at age 2 years. *A*, Sagittal T1-weighted image shows shrunken appearance of the vermis, with commensurate folial volume loss and fissural enlargement involving the anterior lobe and declive (*thick arrows*) and flattened inferior vermis (*thin arrows*). The pontine protuberance is small (*arrowheads*). *B*, Coronal T2-weighted and (*C*) FLAIR images show shrunken, hyperintense hemispheric cerebellar cortex bilaterally; the cerebellar white matter is also mildly hyperintense compared with supratentorial white matter, resulting in a “bright cerebellum” appearance. *D*, Coronal ADC map shows the cerebellum is hyperintense compared with the supratentorial brain, consistent with facilitated diffusion. *E*, ¹H-MRS findings; single-voxel PRESS technique at TE 23 ms. Upper right coronal FLAIR image shows placement of a 18 × 18 × 18 mm voxel on right cerebellar hemisphere. Corresponding spectrum shows markedly reduced NAA peak, mildly reduced Cho, and elevated inositol (mI and sI) resonances. There is a high alpha-Glx peak at 3.8 ppm, perhaps in relation to hepatic dysfunction in this patient. Glx indicates glutamine/glutamate complex.

follow-up, with a more rudimentary appearance of the individual folia and not particularly enlarged fissures (Figs 1 and 2). Only in 1 case (case 5), in which the degree of cerebellar volume loss was very mild, the cerebellar vermis had a near-normal appearance with only mild folial volume reduction at presentation, which progressed on follow-up.

A second characteristic feature consisted of cerebellar cortical hyperintensity on long TR (ie, T2-weighted and FLAIR) images (Fig 1), observed at presentation in 3 cases (cases 2, 3, 4) and on follow-up in the other 2. The subcortical white matter also appeared mildly hyperintense, especially in the FLAIR images, resulting in a globally hyperintense appearance of the cerebellum in 4 patients (cases 1–4) (Figs 1–3). The middle cerebellar peduncles had normal signal intensity in all cases. The dentate nuclei were hyperintense in 1 patient (case 5). DWI consistently showed increased diffusion within the cerebellum, involving both the cortex and subcortical white matter.

The brain stem appeared abnormal in 4 patients (cases 1–4). The abnormality consisted of a reduced bulge of the pontine protuberance (Figs 1–3) that was progressive on follow-up studies in 3 cases, paralleling cerebellar volume loss (Figs 2 and 3). There was a pontine “hot cross bun” sign in 1 case (case 3), consisting of T2-hyperintense transverse fibers

and median raphe, as seen in olivopontocerebellar atrophy⁹ (Fig 3). In case 5, which was characterized by a mild degree of cerebellar atrophy and localized T2/FLAIR cortical hyperintensity, the pons remained normal at 2-year follow-up.

Supratentorial abnormalities involved the white matter in 2 cases. In case 1, myelination was delayed at age 11 months. In case 3, white matter volume loss and gliosis, corpus callosum atrophy, and cortical atrophy were found at presentation and significantly progressed on follow-up (Fig 3). Both patients had a significant degree of ventriculomegaly as a consequence of their supratentorial volume loss.

¹H-MRS was interpretable in only 3 cases (cases 3, 4, 5), whereas quality was deemed insufficient in 1 (case 2) because of motion artifacts. The most significant finding consisted of reduced NAA/Cr ratios, which was particularly severe in cases 3 and 4, where the NAA peak was barely detectable (Fig 1); additionally, increased mIns was detected in 2 cases (cases 4, 5). In 1 case (case 4), prominent peaks at 3.36 and 3.8 ppm were found; these were automatically assigned to sI and the alpha-resonances of glutamine and glutamate, respectively (Fig 1).

Discussion

In CDG-1a patients, MR imaging typically shows a small cerebellum, variably designated as CH, olivopontocerebellar hy-

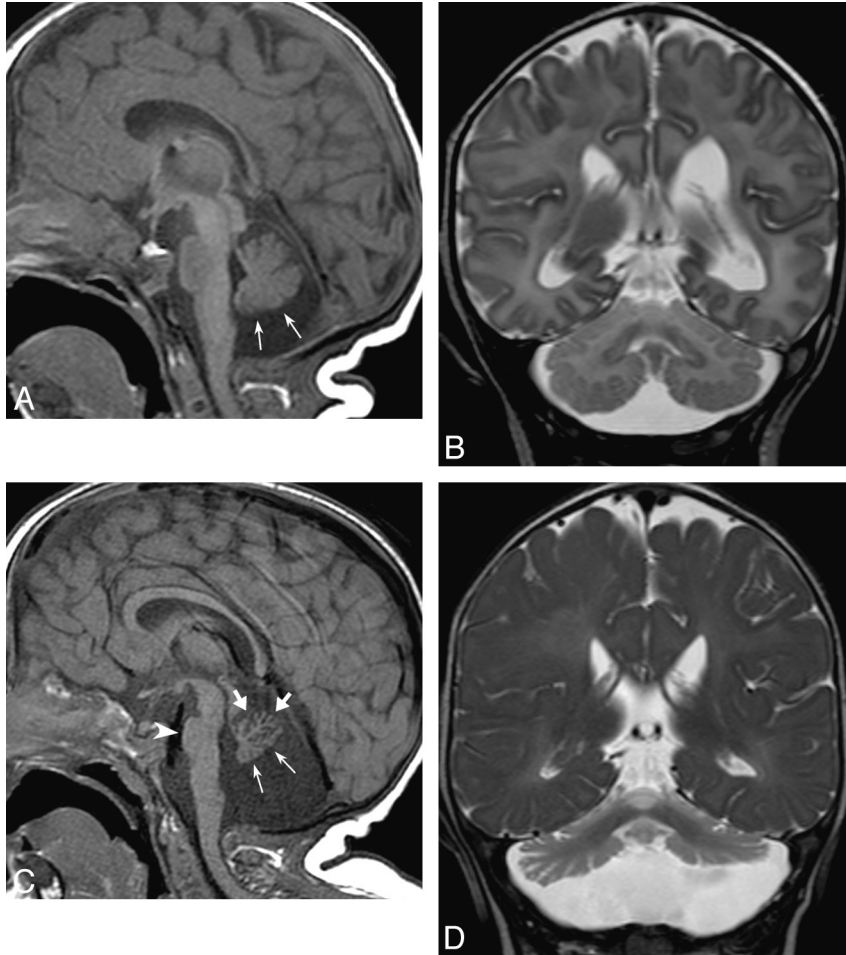


Fig 2. Evolution of findings in CDG-1a; case 1 at age 12 days (A and B) and 11 months (C and D). At presentation, sagittal T1-weighted image (A) shows mild hypoplasia of the inferior vermis (*thin arrows*); the pons and superior vermis appear normal. Coronal T2-weighted image (B) shows normal cerebellar hemispheres. At 11-month follow-up, sagittal T1-weighted image (C) shows considerable volume loss of the vermis. Notice, in particular, atrophic involution of the anterior lobe and declive (*thick arrows*), with corresponding fissural enlargement, whereas the inferior vermis retains a flattened appearance (*thin arrows*), with not so large fissures. The pontine protuberance is also diminished in size (*arrowhead*). Coronal T2-weighted image (D) also shows reduced size of both cerebellar hemispheres. The cerebellar cortex is hyperintense.

poplasia, and CA in the literature.³⁻⁷ Cerebellar MR spectroscopy findings have not been reported to our knowledge, though 1 report showed decrease in the NAA peak in supratentorial acute stroke regions.³

Theoretically, the differentiation between CA and CH should be straightforward. CA is a progressive neurodegenerative condition in which an initially normal cerebellum displays progressive volume loss, with interfolial spaces eventually appearing larger than the folia. Conversely, CH is a congenital condition characterized by incomplete development of the cerebellum, in which the fissures are of normal size compared with the folia.¹⁰ In practice, such differentiation is much less easy to achieve, particularly when a single MR imaging study is available. In our series, all patients exhibited a variably severe volume loss of the cerebellum at presentation, with involvement of both the vermis and the cerebellar hemispheres, which further progressed on follow-up. Close scrutiny of vermian morphology revealed that, in most cases, the inferior vermis had a rudimentary, flattened appearance in the early stages, consistent with inferior vermis hypoplasia; on the other hand, atrophy became prominent in the superior vermis at later stages, but typically in the first 2 years of life. This suggests that neurodegeneration occurs early, when the external granule

layer, which appears at the end of the embryonic period and persists up to 2 years after birth,¹¹ is still playing an active germinal role and the development of the cerebellum is still incomplete. Thus, cerebellar involvement in CDG-1a is probably best described as a combination of CA and CH, similar to pontocerebellar hypoplasia and other putative prenatal-onset degenerative disorders.^{10,12,13}

A consistent, striking finding in our series was the presence of high T2/FLAIR signal intensity of the involved cerebellar cortex and, often, the subcortical white matter. To the best of our knowledge, this is a novel finding in CDG-1a, which we believe may be important in the differential diagnosis. In fact, CA is a nonspecific radiologic finding in children with a host of different causes, including genetic and acquired conditions, with different prognoses and, in some instances, therapeutic strategies; a pattern-recognition approach may therefore critically restrict the differential diagnosis and prompt specific laboratory and genetic studies. To this end, Poretti et al¹² identified 5 subgroups of CA, namely, 1) isolated CA, comprising ataxia-telangiectasia, late-onset GM2 gangliosidosis, and ataxia-oculomotor apraxias; 2) CA and hypomyelination, including Pelizaeus-Merzbacher disease, Salla disease, leukoencephalopathy

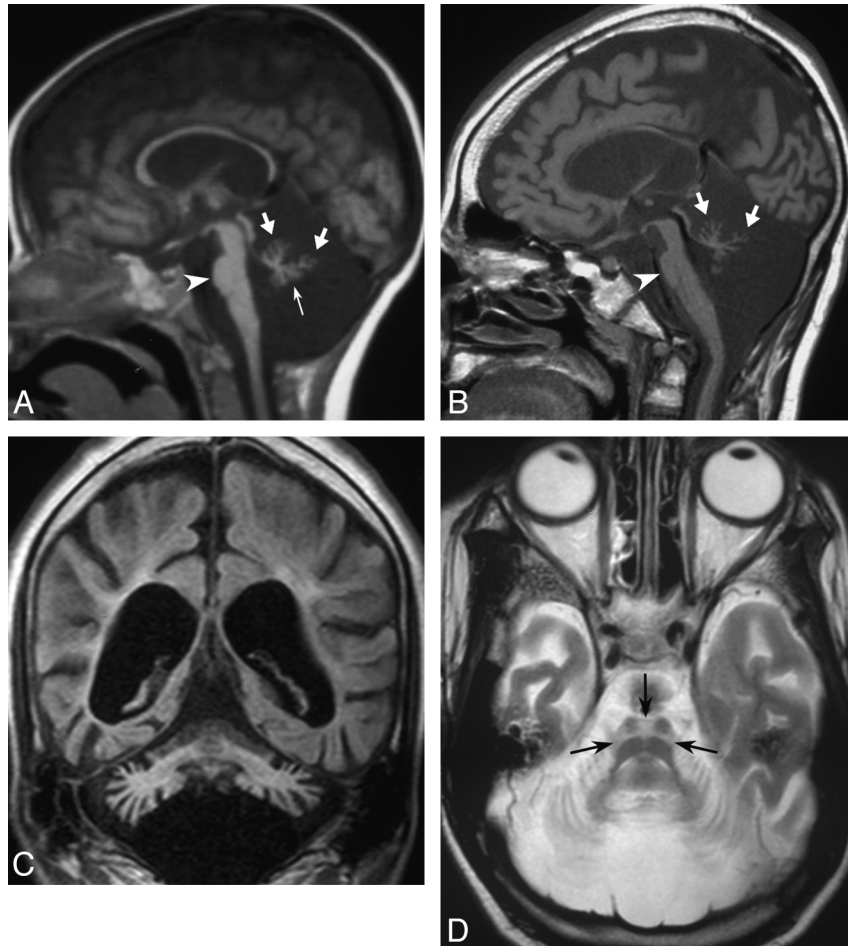


Fig 3. Long term follow-up in CDG-1a; case 3 at age 2 years (A) and 16 years (B–D). At presentation, sagittal T1-weighted image (A), performed 20 years ago on a 0.5T MR unit, shows markedly small cerebellar vermis, with larger fissures superiorly (*thick arrows*) compared with a flattened appearance inferiorly (*thin arrow*). The pons is small (*arrowhead*). After 14 years, sagittal T1-weighted image (B) shows further volume loss involving both the superior (*thick arrows*) and inferior vermis. The pontine protuberance is further reduced (*arrowhead*), and the corpus callosum is markedly thinned. Coronal FLAIR image (C) shows hyperintense, atrophic cerebellum, supratentorial atrophy with white matter gliosis, and ventricular enlargement. Axial T2-weighted image (D) shows the pontine “hot cross bun” sign (*arrows*) and cerebellar cortical atrophy.

with ataxia, hypodontia and hypomyelination, and hypomyelination with atrophy of the basal ganglia and cerebellum; 3) CA and progressive white matter abnormalities, comprising neuronal ceroid lipofuscinoses, Niemann-Pick disease type C, dentatorubral-pallidoluysian atrophy, vanishing white matter disease, and L2-hydroxyglutaric aciduria; 4) CA and basal ganglia involvement, including Kearns-Sayre syndrome and other mitochondrial disorders, Cockayne syndrome, Wilson disease, and 3-methylglutaconic aciduria; and 5) CA with cerebellar cortex hyperintensity. This latter category mainly comprises infantile neuroaxonal dystrophy, Marinesco-Sjogren syndrome, and mitochondrial disorders, other than acquired forms of CA, such as those following viral cerebellitis or exposure to exogenous toxic agents. We suggest that CDG-1a should also be included in the category of CA with cerebellar cortex hyperintensity; in such a context, a globally (rather than just cortical) hyperintense cerebellum on FLAIR, with evidence of volume loss in a patient presenting in the first 2 years of life, seems an important feature. In the absence of histologic verification, the cause of cerebellar hyperintensity remains speculative. We surmise a combination of astrogliosis, neuronal loss, and wrinkling of the cortex occurs,

as suggested by ^1H -MRS findings of reduced NAA/Cr and increased mIns concentrations that presumably reflect neuronal loss and astrogliosis, respectively.

Another important, albeit not constant, aspect in our series was represented by a small pontine protuberance. This finding was progressive in most cases, paralleling the progression of cerebellar volume loss and contradicting the increase in size that normally occurs during infancy.⁸ A small pons is a remarkable finding in the setting of CA, in that most hereditary forms of CA do not lead to significant brain stem atrophy, even in an advanced stage, with the notable exception of late-stage spinocerebellar ataxias and the group of pontocerebellar hypoplasias.¹² The addition of CDG-1a to this group confirms that this is a form of early-onset neurodegenerative disorder.

The authors acknowledge that this study may be limited by intra- or interobserver variations due to our use of 2 unblinded observers to record all findings by consensus. Furthermore, standardized measurement techniques, including brain stem and cerebellar morphometry and ADC value determinations, could not be performed in all cases, which may have increased the risk of an inaccurate or biased interpretation of findings.

To summarize, our small sample of CDG-1a patients con-

sisted of children presenting, within the first 2 years of life, with variably severe but consistent MR imaging features of a small, hyperintense cerebellum, often associated with a small pons. This association seems to be peculiar in the large field of cerebellar atrophies and may prove useful in addressing the differential diagnosis by prompting specific laboratory tests, thereby saving time and costs. MR imaging findings, supported by ¹H-MRS findings of reduced NAA/Cr and increased inositol resonances, support the hypothesis that CDG-1a is an early-onset neurodegenerative disorder in which cerebellar atrophy and hypoplasia coexist.

References

1. Jaeken J, Artigas J, Barone R, et al. **Phosphomannomutase deficiency is the main cause of carbohydrate deficient glycoprotein syndrome with type I iso-electrofocusing pattern of serum sialotransferrins.** *J Inherit Metab Dis* 1997; 20:447–49
2. Sparks SE, Krasnewich DM. **PMM2-CDG (CDG-1a).** In: Pagon RA, Bird TD, Dolan CR, et al, eds. GeneReviews [Internet]. Seattle: University of Washington; 1993- 2005 Aug 15 [updated 2011 Apr 21].
3. Pearl PL, Krasnewich D. **Neurologic course of congenital disorders of glycosylation.** *J Child Neurol* 2001;16:409–13
4. Antoun H, Villeneuve N, Gelot A, et al. **Cerebellar atrophy: an important feature of carbohydrate deficient glycoprotein syndrome type 1.** *Pediatr Radiol* 1999;29:194–98
5. Jensen PR, Hansen FJ, Skovby F. **Cerebellar hypoplasia in children with the carbohydrate-deficient glycoprotein syndrome.** *Neuroradiology* 1995;37: 328–30
6. Steinlin M, Blaser S, Boltshauser E. **Cerebellar involvement in metabolic disorders: a pattern-recognition approach.** *Neuroradiology* 1998;40:347–54
7. Aronica E, van Kempen AA, van der Heide M, et al. **Congenital disorder of glycosylation type Ia: a clinicopathological report of a newborn infant with cerebellar pathology.** *Acta Neuropathol* 2005;109:433–42
8. Raininko R, Autti T, Vanhanen SL, et al. **The normal brain stem from infancy to old age.** *Neuroradiology* 1994;36:364–68
9. Shrivastava A. **The hot cross bun sign.** *Radiology* 2007;245:606–07
10. Boltshauser E. **Cerebellum—small brain but large confusion: a review of selected cerebellar malformations and disruptions.** *Am J Med Genet A* 2004; 126A:376–85
11. Lemire RJ, Loeser JD, Leech RW, et al. **Normal and abnormal development of the human nervous system.** Hagerstown: Harper and Row; 1975
12. Poretti A, Wolf NI, Boltshauser E. **Differential diagnosis of cerebellar atrophy in childhood.** *Eur J Paediatr Neurol* 2008;12:155–67
13. Barkovich AJ, Millen KJ, Dobyns WB. **A developmental and genetic classification for midbrain-hindbrain malformations.** *Brain* 2009;132:3199–230